12 Surface Physics

T. Greber, M. Hengsberger, S. Berner, C. Galli Marxer, J. H. Dil, H. Yanagisawa, M. Morscher, T. Brugger, F. Meier, D. Leuenberger, A. Devizis, T. Mattle, S. Roth, J. Schmidlin, M. Klöckner, J. Osterwalder

In the surface physics group model systems of well defined surfaces and interfaces are systematically studied in order to address fundamental issues that are relevant for nanoscience and nanotechnology. Our laboratory is well equipped for the preparation and characterization of clean surfaces, metal and molecular monolayer films, as well as self-assembling nanostructures, all under ultrahigh vacuum (UHV) conditions. Experimental techniques available to us include x-ray photoelectron spectroscopy (XPS) and diffraction (XPD), angle-resolved photoemission spectroscopy (ARPES), two-photon photoemission (2PPE) using femtosecond laser pulses, low-energy electron diffraction (LEED) and scanning tunneling microscopy (STM). During this past year, a new variable-temperature STM could be purchased, partly funded by the R'Equip program of the Swiss National Science Foundation (SNF). A new UHV system was designed and built, and the instrument was successfully commissioned. At the nearby Swiss Light Source (SLS) we operate two more photoemission spectrometers, one for spin-resolved Fermi surface mapping and one for photo-electron diffraction and holography. A growing network of national and international collaborations expands this set of experimental techniques and provides us also with the necessary theoretical support.

The research carried out during the report period can be grouped into four topics:

- **Monolayer films of hexagonal boron nitride on metal surfaces**
  The boron nitride nanomesh continued to be one of our major research interests, funded in part by the SNF and the EU (FP6-STREP "NanoMesh"). This one atom thick layer of boron nitride on Rh(111) surfaces, which was discovered some years ago in our group (1), exhibits a very regular hexagonal corrugation pattern with 2 nm wide depressions ("holes") and a periodicity of 3.2 nm, giving the surface a mesh-like appearance in STM images. Its periodicity and atomic structure are now fairly well understood (2; 3; 4), a further structural refinement by means of surface x-ray diffraction (SXRD) is currently ongoing in collaboration with the SXRD group of the SLS. After establishing the ability of the nanomesh to trap naphthalocyanine molecules within the holes, thus forming self-assembled molecular arrays covering macroscopic surface areas (4), we could now contribute to the understanding of the trapping mechanism that keeps the molecules in place (see Sec. 12.1 and Ref. (5)). These studies were extended to other molecules, like copper phthalocyanine and more recently Co carbonyls, the latter with a view of producing Co metal nanoclusters within the nanomesh holes. Preliminary results indicate that Co atoms remain on the surface and form clusters, while the carbonyl groups desorb when the warm nanomesh surface is exposed to a flux of molecules. One of the most remarkable properties of the nanomesh is its robustness when exposed to air and even when immersed in water (6). Within a Master thesis project (T. Mattle), the stability range under electrochemical conditions has been further characterized at EMPA Thun, and preliminary studies of molecular adsorption from the liquid phase are ongoing.

- **Ultrafast processes at surfaces**
  From the laser laboratory, which is located adjacent to the lab housing the photoelectron spectrometer, femtosecond laser pulses can be coupled through a hole in the wall into the photoemission chamber. With this setup, 2PPE experiments can be performed, exploiting also the angular degrees of freedom of the UHV sample goniometer. This has been demonstrated in a recent publication on photoemission momentum mapping and wave function analysis of surface and bulk states on Cu surfaces (7). In a recent Master project (D. Leuenberger), the poorly understood *ultrafast demagnetization* of a Ni surface by fs-laser pulses, previously observed by other groups in optical (8) and photoemission (9) experiments, had been addressed in a new approach. The clean Ni(111) surface is protected by a single boron nitride monolayer, providing at the same time a strongly resonant emission peak in 2PPE spectra (10). In principle, this resonance should be sensitive to changes in the Ni band structure associated with the demagnetization process. The experiments have so far produced ambiguous results and the study has been expanded into a PhD project. In a new Master project (S. Roth), we have started an investigation of diamondoid (nano-clusters of diamond) covered Ag surfaces in view of their interesting property of *negative electron affinity* (NEA) (11). Such surfaces have their lowest unoccupied molecular orbital situated above the vacuum energy and show therefore strongly enhanced electron emission upon photo-excitation. Specifically, self-assembled monolayers of thiolated tetramantane molecules that were obtained through a collaboration with Chevron U.S.A. Inc., Richmond CA, were prepared on Ag(111) and are currently being studied by time-resolved 2PPE. In parallel, the group is commissioning a new photoemission spectrometer in the laser lab. This instrument has been moved from PSI to Zürich (courtesy Ch. Quitmann). It contains an ellipsoidal display analyzer (12) and will allow to measure 2PPE momentum distributions very efficiently.

- **Spin-resolved photoemission and momentum mapping**
  After a couple of very difficult years of identifying, characterizing and fixing magnetic shielding problems, our spin-resolved photoemission chamber at the SLS (COPHEE, the complete photoemission experiment) is now working very well. As a first demonstration, the spin polarization and the spin structure of the electronic states in the two surface alloys Bi/Ag(111) and Pb/Ag(111) have been successfully measured (see Sec. 12.2), and a paper has been accepted for publication in Physical Review B. The unique capability of the instrument to resolve all components of the spin polarization vector of the photoelectrons made it possible to introduce a new two-step fitting routine that provides absolute spin polarization vectors for each individual band intersected in a particular measurement. This procedure is crucial when investigating this type of two-dimensional systems where spin-orbit effects lead to complex momentum dependent spin structures (13; 14). With the photoelectron spin as an additional tag in the measurement, spin-split bands with splittings far below the measured line width can be resolved. This has allowed us to see such splittings in quantum well states within ultrathin Pb layers on Si(111). Comparable to surface states, the space inversion symmetry is broken in these films, and the spin degeneracy of the valence electrons is lifted. The effect is much smaller, though, and first results have shown a splitting of only 15 meV in such films.

- **Further instrumental developments**
  The importance of the electron spin in chemical bonding is obvious (Pauli princi-

ple). For molecules adsorbed on ferromagnetic surfaces, where the absolute spin orientation in spin-split bands can be interchanged by controlling the macroscopic sample magnetization direction, the spin-dependent coupling of molecular orbitals to states of the underlying substrate can be studied. In order to exploit the versatile preparation and characterization environment of our photoelectron spectrometer chamber, we have engaged in a development project for a simplified type of spin detector that is compatible with the existing hemispherical electron analyzer. In this new type of Mott detector, backscattered high-energy electrons are measured within scintillator crystals. The light pulses are extracted by glass rods out of the UHV. This design avoids the complex high-voltage operation of the preamplifiers. A first prototype of the device has been built and will soon be ready for testing.

In conjunction with the nanomesh project, the interest arises whether individual molecules trapped within nanomesh pores can be addressed via optical fluorescence. In order to have a substantial fluorescence yield, excited molecular states have to be long lived, which is not obvious for molecules adsorbed on a metal surface, where many de-excitation channels exist. It is therefore crucial to establish whether the presence of the single-layer boron nitride dielectric provides sufficient decoupling from the underlying Rh surface. Within a Master project (J. Schmidlin), our room temperature STM has been equipped with a detector for recording fluorescence photons excited locally by the tunneling current from the tip. Preliminary measurements show clear photon signals correlating with the tunneling voltage.

In the following, two highlights of last year's research are presented in more detail.

12.1 Boron nitride nanomesh: trapping molecules with dipole rings

In collaboration with: Peter Blaha and Robert Laskowski, Institut für Materialchemie, Technische Universität Wien, A-1060 Vienna, Austria.

The control of the mobility of single atoms or molecules on surfaces is of key importance in nanotechnology. For efficient immobilization or trapping, the bonding has to compromise between bonding strength and deterioration of the specific function of a single molecule, which relies on a minimal coupling to the degrees of freedom of the support. Surface dipoles, which contribute strongly to the bonding of polarizable entities, should lead to lateral immobilization as soon as they also exhibit in-plane components. In this respect, a ring geometry of in-plane dipoles appears most attractive for complete confinement of molecules within a nanometer-size space. The mesh-like monolayer structure of hexagonal boron nitride on Rh(111) (1) represents a perfect realization of a dense layer of such dipole rings with diameters of 2 nm. This is demonstrated by the adsorption of highly polarizable Xe atoms, and by using photoemission from shallow Xe core levels as a sensitive probe for the electrostatic energy landscape on this layer.

It is now established that the h-BN nanomesh on Rh(111) or Ru(0001) is a single sheet of hexagonal boron nitride, where 13x13 BN units form a coincidence lattice with 12x12 substrate unit cells (2; 3; 4; 15). Two distinct BN regions were found within the sp^2-bonded network of h-BN: A closely bound region assigned to the "holes" in the nanomesh and a loosely bound region assigned to the "wires" (see Fig. 12.1) (3; 4; 15). Theory confirmed the experimentally observed electronic structure and showed the sp^2 derived BN σ-band density of states of the holes and the wires to be quasi rigidly shifted with respect to each other by about 1 eV (3). This suggests that a signi ficant

portion of the h-BN σ-band shift is related to electrostatics, i.e. to different work functions of the wires and the holes. The accompanying local vacuum level misalignment imposes electric fields and leads to lateral polarization within the h-BN sheet. This is described with dipole rings, which in turn offer a natural explanation for an enhanced immobilization of molecules. Fig.12.2 shows valence band photoemission data from Xe on h-BN/Rh(111) for different Xe coverages. It is seen that the Xe atoms first occupy sites in the holes and then start to cover wire- and further hole-sites within the nanomesh unit cell. The Xe 5p binding energy difference of 0.3 eV between Xe in the holes and Xe on the wires corresponds to the difference of the electrostatic potential at the sites of the Xe cores, 2Åabove the surface. This is rationalized by in plane dipoles on rings located at the rims of the holes. The potential energy landscape, where the holes attract electrons, is confirmed by density functional theory calculations within a super-cell with more than thousand atoms.

Thermal desorption spectroscopy allows to determine the site specific Xe desorption energies. It is found that 12 Xe atoms in the nanomesh unit cell that were located in the holes, have a desorption energy which is 25 meV larger than that of the 42 other Xe atoms in the nanomesh unit cell with a full monolayer (182±0.05 meV). We expect dipole rings also to occur in other dislocation networks and that this concept will improve the understanding of two-dimensional templates for supramolecular structures.

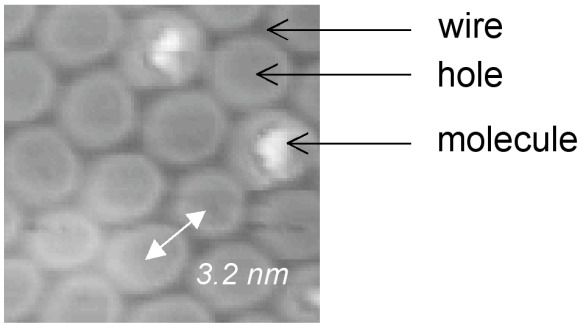

Figure 12.1: Scanning tunneling microscopy image of h-BN/Rh(111). About 20 unit cells with a lattice constant of 3.2 nm are shown. The two distinct regions of the wires (dark) and the holes (bright) are marked. Two holes are occupied by Cu-phthalocyanine molecules.

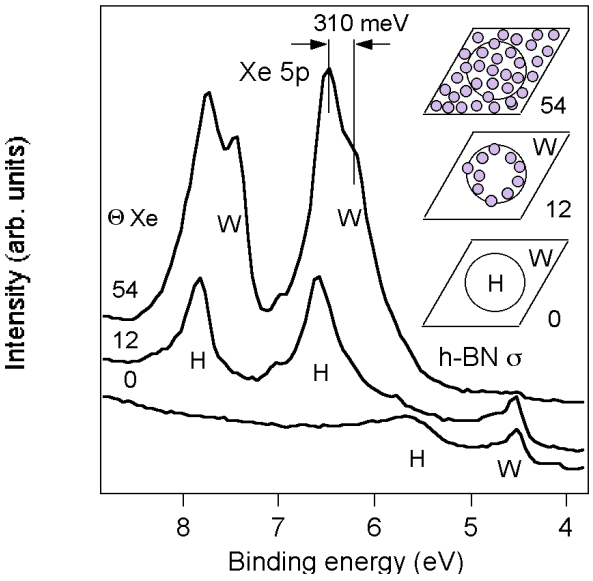

Figure 12.2: Photoemission spectra ($\hbar\omega$=21.2 eV) for three different Xe coverages on h-BN nanomesh. Θ Xe is the number of Xe atoms per unit cell. H stands for hole, W for wire. When Xe is in the holes the H-σ-bands are suppressed. The three icons mimic the nanomesh unit cell and the location of the Xe atoms. The Xe 5p doublet is also split in a H and a W contribution. The energy difference of 310 meV corresponds to the electrostatic potential-energy difference between the Xe cores on top of the wires and the holes.

12.2 Understanding and tuning the electron spin at surfaces

In collaboration with:
Luc Patthey, Swiss Light Source, Paul Scherrer Insititute, 5232 Villigen, Switzerland.

Methods that allow to control and measure the electron spin, or the average of a certain quantity of spins, have received growing attention in the last few years. In spintronics, the spin field-effect transistor as proposed by Datta and Das (16), which relies on the Rashba-Bychkov effect (17) (henceforth Rashba effect), is one of the key elements. The basis of the Rashba effect lies in the breaking of the crystal symmetry at the surface and the resulting absence of space inversion symmetry. For a parabolic band this will produce two parabola that are split in momentum and cross at the centre of the Surface Brillouin zone. The size of this splitting is determined by the magnitude of the potential gradient at the surface and the atomic number Z of the atoms involved. In order to utilize the Rashba effect the splitting of the two bands has to be large compared to the other energy scales in the system. Recently, a very large band splitting was reported in the two surface alloys Bi/Ag(111)$\sqrt{3} \times \sqrt{3}$ ($R30°$) and Pb/Ag(111)$\sqrt{3} \times \sqrt{3}$ ($R30°$) (18; 19), henceforth referred to as Bi/Ag(111) and Pb/Ag(111). The spin integrated band structure can roughly be explained by a Rashba type spin-orbit splitting of the Bi (or Pb) induced surface states. In these systems the Rashba effect is strongly enhanced due to an additional reduction of the surface symmetry caused by the $\sqrt{3} \times \sqrt{3}$ ($R30°$) surface reconstruction and due to the corrugation of the surface (20). Furthermore it has been proposed that the symmetry of the individual bands plays a crucial role in the Rashba effect.

Spin and angle resolved photoemission spectroscopy (SARPES) data were obtained for the Bi/Ag(111) and Pb/Ag(111) surface alloys using the COPHEE spectrometer located at the surface and interface spectroscopy beamline at the Swiss light source (21). This spectrometer is capable of measuring the spin polarization along three orthogonal directions in real space for any point in reciprocal space (22). This means that all the quantum numbers of a photoemitted electron can be obtained. In order to harness the amount of information obtained in this manner a novel two step fitting routine has been developed. Using this routine the magnitude and orientation of the spin polarization vector in three dimensional space can be obtained for individual bands. The usefulness and necessity of this approach is illustrated in Fig. 12.3. Due to their large number of bands and complex band structure these surface alloys provide ideal test cases. An additional benefit of this procedure is that bands which can normally not be resolved in spin integrated photoemission are easily separated using the spin as an additional tag of individual bands. Our data confirm that the orientation of the spin polarization vector depends on both the orientation of the potential gradient and the orbital symmetry of a state. This information is typically not accessible in spin integrated ARPES and can be used to verify ab-initio density functional theory calculations. Although the measured spin polarization is usually less than one due to overlapping bands and an unpolarized background, our analysis shows that the true polarization of individual bands is either zero or one. This finding sheds a new light on previous publications in the field, both theoretical and experimental. In order to standardize the results of spin resolved measurements and theoretical treatments, we suggest to focus on the direction of the spin polarization vector rather than the relative magnitude of the polarization along a coordinate system, especially for non magnetic samples. Building on the understanding of the electron spin behaviour at surfaces obtained from these experiments we can now explore some possibilities to tune electron spins in artificial systems prepared by standard surface science procedures.

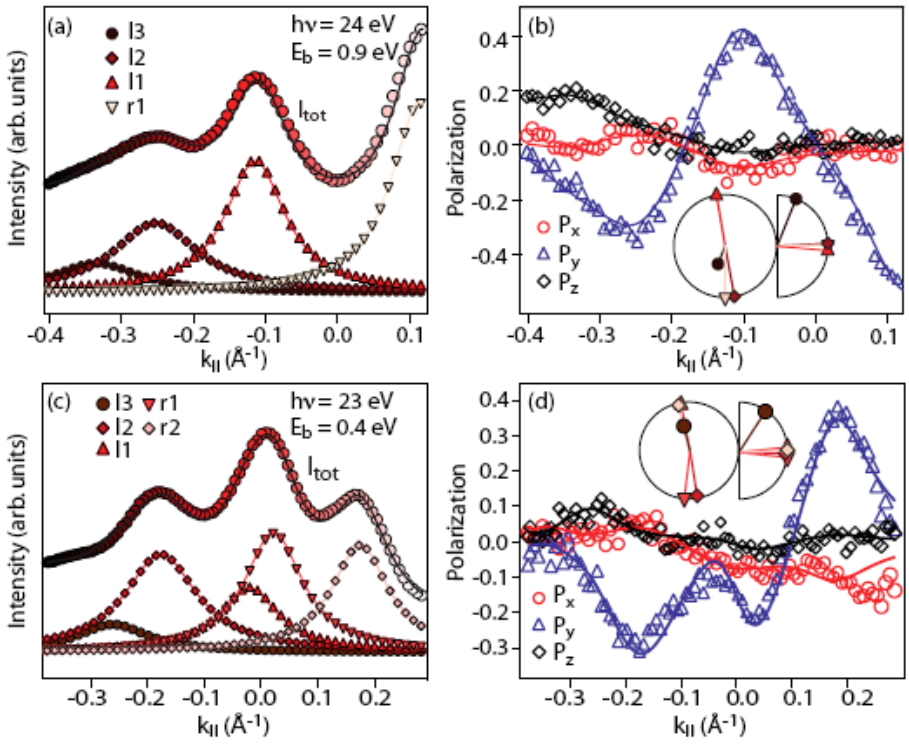

Figure 12.3:
Photoemission momentum distribution curves measured on Bi/Ag(111) at a binding energy E_B = 0.9 eV with $\hbar\omega$ = 24 eV (top panels) and at E_B = 0.4 eV with $\hbar\omega$ = 23 eV (bottom panels) along the $\overline{\Gamma K}$ direction of the surface Brillouin zone (from Ref. [21]).
(a) and (c):
spin integrated intensities and the Lorentzian peaks of the fit. The solid line is the total intensity fit.
(b) and (d):
measured (symbols) and fitted (solid lines) spin polarization curves from the MDC. The statistical errors are smaller than the symbol size. The insets visualize the in-plane and out-of-plane spin polarization components obtained from the polarization fit, where the symbols refer to those in (a) and (c).

[1] M. Corso, et al., Science 303, 217 (2003).
[2] O. Bunk et al., Surf. Sci. 601, L7 (2007).
[3] R. Laskowski et al., Phys. Rev. Lett, 98, 106802 (2007).
[4] S. Berner et al. Angewandte Chemie Int. Ed. 46, 5115 (2007).
[5] J. H. Dil et al., Science 319, 1824-1826 (2008).
[6] R. Widmer et al., Electrochemistry Commun. 9, 2484 (2007).
[7] M. Hengsberger et al., Phys. Rev. B 77, 085425 (2008).
[8] E. Beaurepaire et al., Phys. Rev. Lett. 76, 4250 (1996).
[9] H. S. Rhie et al., Phys. Rev. Lett. 90, 247201 (2003).
[10] M. Muntwiler et al., Phys. Rev. B 75, 075407 (2007).
[11] W. L. Yang et al., Science 316, 1460 (2007).
[12] T. Dütemeyer et al., Rev. Sci. Instrum. 72, 2638 (2001).
[13] S. LaShell et al., Phys. Rev. Lett. 77, 3419 (1996).
[14] M. Hoesch et al., Phys. Rev. B 69, 241401 (2004).
[15] A. Goriachko et al. Langmuir, 23, 2928 (2007).
[16] S. Datta and B. Das, Appl. Phys. Lett. 56, 665 (1990).
[17] Y.A. Bychkov and E.I. Rashba, JETP Lett. 39, 78 (1984).
[18] C. R. Ast et al., Phys. Rev. Lett. 98, 186807 (2007).
[19] D. Pacile et al., Phys. Rev. B 73, 245429 (2006).
[20] G. Bihlmayer et al., Phys. Rev. B 75, 195414 (2007).
[21] F. Meier et al., Phys. Rev. B (in press); cond. mat. arXiv:0802.1125.
[22] M. Hoesch et al., J. Electron Spectrosc. Relat. Phenom. 124, 263 (2002).